PETROPHYSICS, VOL. 59, NO. 4 (AUGUST 2018); PAGES 496–510; 16 FIGURES. DOI: 10.30632/PJV59V4-2018a5

Production Monitoring Using Next-Generation Distributed Sensing Systems

G. Naldrett[1], C. Cerrahoglu[1], and V. Mahue[1]

ABSTRACT

Distributed fiber-optic sensing, and specifically the introduction of intelligent distributed acoustic sensing (DAS), has gained the attention of production engineers with the promise of a versatile and cost-effective decision-support tool. These systems can either be permanently installed, or temporarily deployed using diverse types of intervention systems.

This article covers the principles of flow allocation using distributed sensing and show how these can be used and combined to identify fluid-entry points, quantify production and identify fluid phases. We will describe the methods used to improve quantitative interpretation from distributed sensing, especially the use of phase-coherent DAS for quantitative measurement of sound speed and its use in analyzis of flow velocity and fluid phase.

While early DAS systems were previously limited in their flow-detection thresholds we have recently introduced a new sensing system, bringing a 20dB (100×) improvement in signal-to-noise. This offers a significant improvement in measurement and associated interpretation capability.

INTRODUCTION

Distributed fiber-optic sensors were invented in the 1980s (Hartog, 1983) and introduced into the oilfield in the 1990s. The initial areas of interest, and commercially available technologies, were related to distributed temperature sensors (DTS) and distributed strain sensors (DSS). DTS was applied to leak detection, flow profiling and steamflood-monitoring applications (Smolen and van der Spek, 2003). DSS focussed mainly on wellbore integrity, monitoring strain induced on wellbore casings (Li et a., 2004). Some research has also been carried out on the use of DSS systems for distributed pressure sensing, but to date, these have not delivered the required performance and reliability for commercial application.

In the late 1990s, research was carried out on the use of optical fibers for distributed vibration sensing (Shatalin et al., 1998), which would later lead to the development of DAS. While there is no industry consistency in naming conventions, in this article we will describe DAS systems as those that are able to measure the acoustic amplitude, phase and frequency of disturbances along a fiber. Distributed vibration sensing (DVS) systems are typically able to detect and locate a disturbance but may not be able provide a measurement response proportional to the magnitude of the disturbance. DVS systems also typically lack acoustic-phase coherence. This means that while a DVS system can detect the disturbance, it cannot tell if the disturbance is extending or compressing the fiber. Most of the spectral content is therefore lost and the user will be unable to recreate the original acoustic information from a DVS recording.

METHODS OF OPERATION

Distributed temperature sensors use a laser to launch of short pulse of narrow-band light into an optical fiber. As this short pulse of light travels through the fiber a small amount is backscattered and returned to the interrogator unit. Because the speed of light in the fiber is known, it is possible to analyze the backscatter spectrum every few centimeters along the fiber. By analyzing the ratio of the Stokes and anti-Stokes signal in the backscatter signal it is possible to calculate the temperature along the entire length of fiber (Smolen and van der Spek, 2003). Temperature measurements can be made every 12.5 cm, along the full length of cable, and continuously updated every 1 s. Although DTS technology is now quite mature, advances continue in development of systems with shorter pulse widths, improved optical receivers and more efficient processing. These allow improved spatial resolution, temperature resolution, measurement time, power consumption and operating temperature range. It is now common to be able to resolve temperatures of 0.01°C with spatial resolutions of less than 1 m. There is a relationship between acquisition rate and temperature resolution, with longer acquisition time providing improved resolution. Such relationships should be

Manuscript received by the Editor May 24, 2018; revised manuscript received July 13, 2018; manuscript accepted July 16, 2018.
[1]Silixa, 230 Centennial Avenue, Elstree, WD6 3SN, United Kingdom; Garth.Naldrett@Silixa.com; Vernoique.Mahue@Silixa.com; Cagri.Cerrahoglu@Silixa.com

considered during equipment selection and job planning.

DAS also uses a novel optoelectronics to launch narrow-band laser light into an optical fiber. The resulting modulation of backscattered light is continuously monitored with a resolution that corresponds to small increments in distance measured along the fiber's entire length. As the acoustic field around the fiber exerts tiny pressures, it induces strain onto the fiber. The interrogator is sensitive to the relative strain between two sections of the fiber that are separated by a length *dz*, referred to as the gauge length, as shown in Fig. 1.

The gauge length (*dz)* can be selected according to the application, but is normally in the order of 2, 10, or 20 m. The underlying measurement is effectively a measurement of local relative strain made in a continuously moving window as the laser light moves down the fiber from the instrument to the far end. Measurements are normally made at 25-cm increments along the fiber. The DAS response at each channel and time is linearly proportional to the change in average elongation over the gauge length per time sample at the channel location.

DEPLOYMENT METHODOLOGY

While the DAS technology is less than 10 years old, it has been able to use the same fiber-optic deployment methods developed for the more mature DTS technology. Indeed, it is often beneficial to deploy simultaneously both DAS and DTS in combination as they provide independent, but complimentary information on flow profiles. While DAS and DTS require separate interrogator units, connected to individual fibers, these fibers can be bundled into the same cable. This single cable therefore becomes sensitive to both the acoustic field and thermal sources of the environment, as shown in Fig. 2.

The existing population of permanent downhole fiber cables with multimode fibers, previously installed on casing or tubing strings for DTS purposes, can now also be used for DAS sensing given suitable arrangements within the DAS interrogator. This offers a new range of applications for existing assets. Although DAS systems are designed to operate using single-mode fibers they can be designed to allow similar performance on multimode fibers. Connections between the 9-µm core of the single-mode fiber and 50-µm core of the multimode fiber create additional losses that should be compensated in the power launched in to the multimode fiber. A more complex problem is the modal excitation along a multimode fiber, which can introduce modal noise and, therefore, deteriorate the quality of the measurement. This is especially apparent on longer fiber lengths. By compensating for different mode excitation and propagation a high-quality measurement can be achieved over several kilometers of multimode fiber. Numerous surveys on multimode fibers installed for DTS measurements show equivalent DAS performance when compared with DAS measurements made on single-mode fibers (Allanic, 2013). Lessons learned about cable design, hydrogen-resistant fibers and in-well connections over 20 years of DTS experience have resulted in significant advances in downhole deployment capability and reliability.

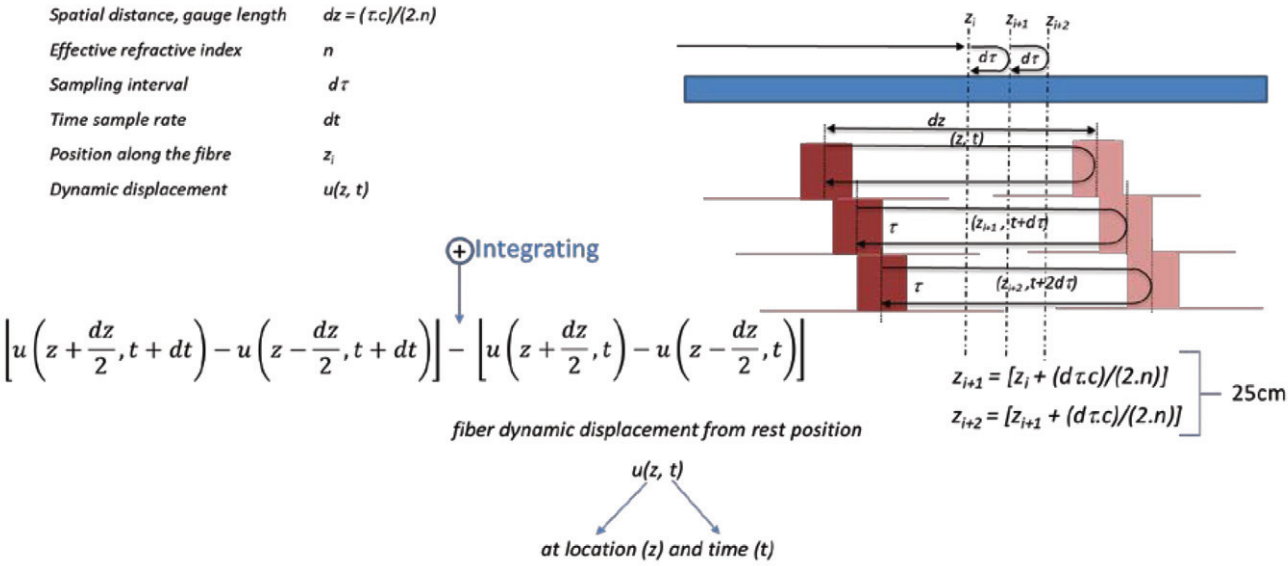

Fig. 1—Illustration of the measurement principles as well as the gauge length along a fiber.

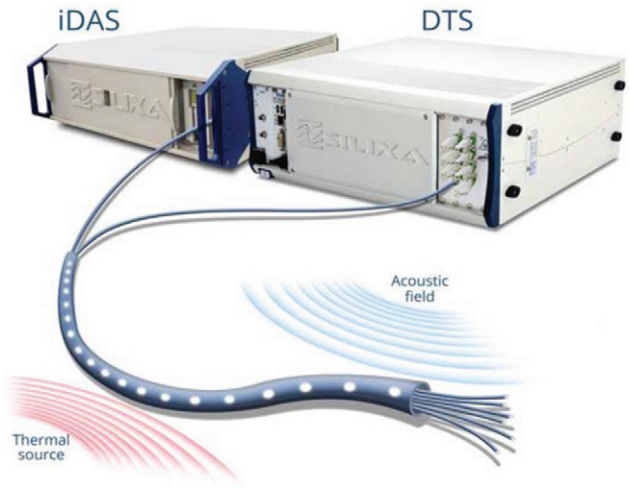

Fig. 2—Simultaneous measurement of distributed temperature and acoustics on a single cable.

Distributed fiber-optic sensing based on DAS and DTS offers a wide range of applications (Fig. 3). In chronological order from well construction these include the monitoring of cement placement and hydration, baseline VSP imaging, crosswell seismic tomography, monitoring of proppant placement, microseismic detection, production flow profiling, wellhead flow measurement, artificial-lift optimization, 4D seismic, right through to well integrity for plug and abandonment planning and execution. This wide range of applications offers significant value creation from a single technology.

Fiber-optic intervention cables have smaller diameters than logging tools, enabling measurements in tight boreholes or restricted completions. Elevated temperatures, or corrosive environments, can also prevent the deployment of logging tools. Fiber cables are more resilient and have been successfully deployed in downhole temperatures up to 280°C (535°F). The fully distributed nature of DAS and DTS allows the entire wellbore to be monitored without moving the toolstring. This complete measurement coverage is useful in identifying crossflows or leaks during bleed downs. This also greatly speeds up wide-aperture VSP surveys.

Fiber-optic intervention cables are also not new to the industry, many wireline cables have been developed and deployed for high-speed communication and tools, such as downhole video (Cobb and Schultz, 1992). An example of a cable designed specifically for distributed sensing is shown in Fig. 4. This cable has been manufactured in lengths up to 7,300 m (24,000 ft) with an outer diameter of 5/16 in., making it compatible with standard wireline pressure-control equipment. Internally, the cable has a #10 AWG conductor allowing it to power or communicate with downhole tools and tractors. There are multiple fibers within the cable enabling simultaneous measurement of DAS and DTS with single-mode and multimode fibers.

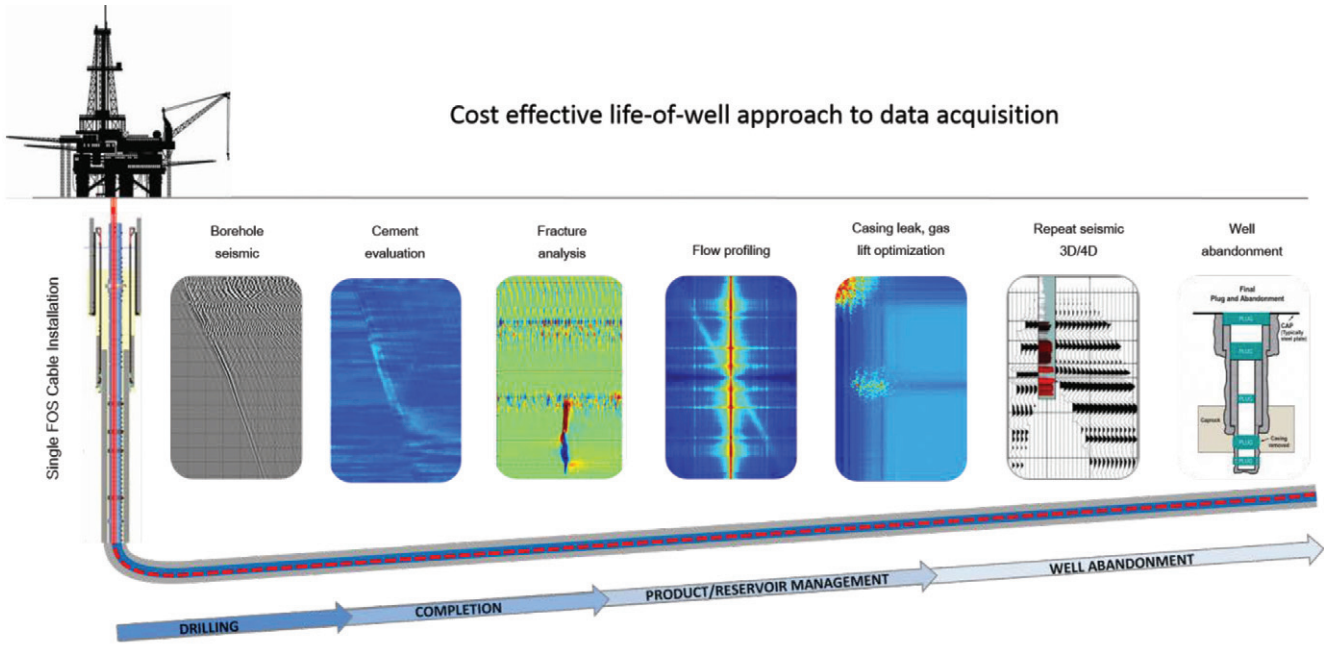

Fig. 3—Range of distributed sensing applications over the life of a field.

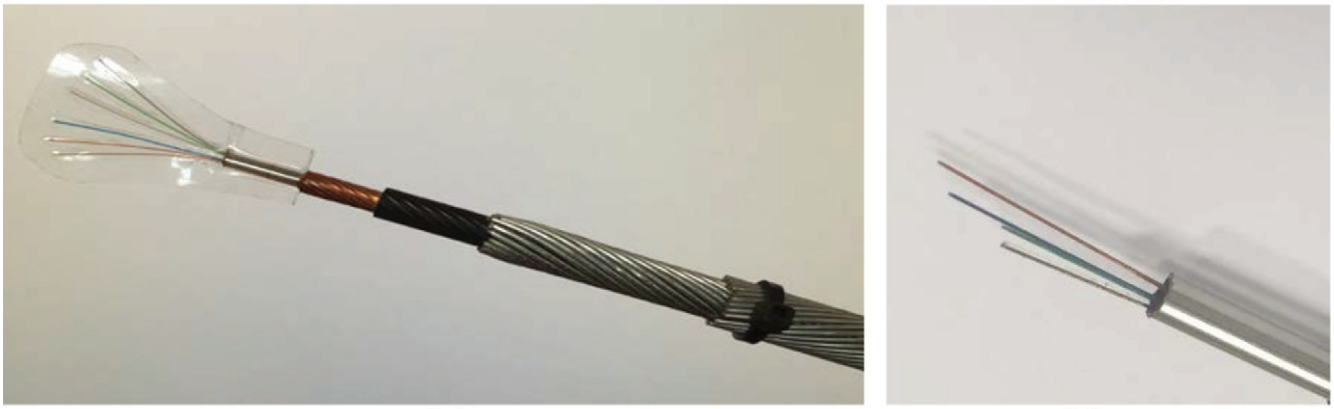

Fig. 4—(a) 5/16-in. Constellation wireline GIPS cable. (b) 1/8-in. slickline cable.

Multiple fibers have also been deployed inside 0.125-, 0.156- and 0.250-in. slickline cables. These are very effective for lower-cost deployments, especially as they are compatible with standard winch units and pressure control. Unfortunately, these cables do not have the same mechanical properties as conventional slickline and have lower breaking strength. They are therefore limited to data acquisition and cannot perform the full set of mechanical operations as conventional solid slickline cables.

Some more novel techniques have been adopted for the deployment of fibers, including the use of synthetic fiber ropes, carbon fiber rods, coiled tubing and minicoils. An offshore minicoil deployment is shown in Fig. 5.

Fig. 5—DAS and DTS surveys through an intervention survey offshore Asia through a minicoil.

The small size and weight of fibers enable new ways to offer wireline services, such as the use of synthetic fibers rather than steel wires for conveyance. These allow more efficient interventions and introduction new tools and techniques for production logging. One innovation is in the form of a winch entirely enclosed inside a pressure vessel (shown in orange in Fig. 6) installed on top of the lubricator as a direct extension of the well. This drastically reduces the complexity and footprint of the operation.

Fig. 6—Fully contained fiber-optic intervention winch unit (courtesy of Capwell).

This miniaturization is made possible using synthetic fiber rope rather than steel wire. The optical fiber embedded inside the rope provides an open platform for optical logging and distributed measurements. This is currently the only way to do well intervention on a live well without any dynamic seals. The rope is constructed from high-modulus, high-tenacity synthetic fibers and is specifically qualified for downhole services. A dual-capstan winch is designed and fitted inside the pressure vessel, which is connected on top of a standard wireline lubricator installed over the Christmas tree. It is internally exposed to well pressure and fluids. This offers a higher return of investment for intervention because of increased operational efficiency and by eliminating the need for complex wireline units and grease injection. The unit is an ideal tool for long-term logging since it has a minimal impact on the facility and no dynamic seals.

BENEFITS OF DISTRIBUTED SENSING WITH FULL WELLBORE COVERAGE

There are many applications that benefit from simultaneous acquisition of data from the full length of the wellbore. One example, taken from an offshore well in the North Sea, is shown in Fig. 7 (Johannessen et al., 2012). In this example, the fiber-optic cable was deployed across a gas-lift valve, located at a measured depth of 2,200 m, while the cable was deployed to a depth of 3,300 m.

During production, it was seen from the full-frequency-band amplitude (Fig. 7) that the well's behavior was unstable. We see acoustically quiet events occurring approximately every 450 s at the location of the gas-lift valve. We believe this is when the gas-lift valve shuts for a few seconds. The events move up the wellbore at a velocity of 2.1 m/s, consistent with the wellbore flow velocity.

With the distributed measurements it was possible to quickly locate the source of instability, in this case the slugging gas-lift valve. A logging tool may have required multiple passes over all gas-lift valves to determine the source of instability or slugging. This is even more complex if the engineer suspects the multiphase fluid behavior to be the source of instability rather than the gas-lift system.

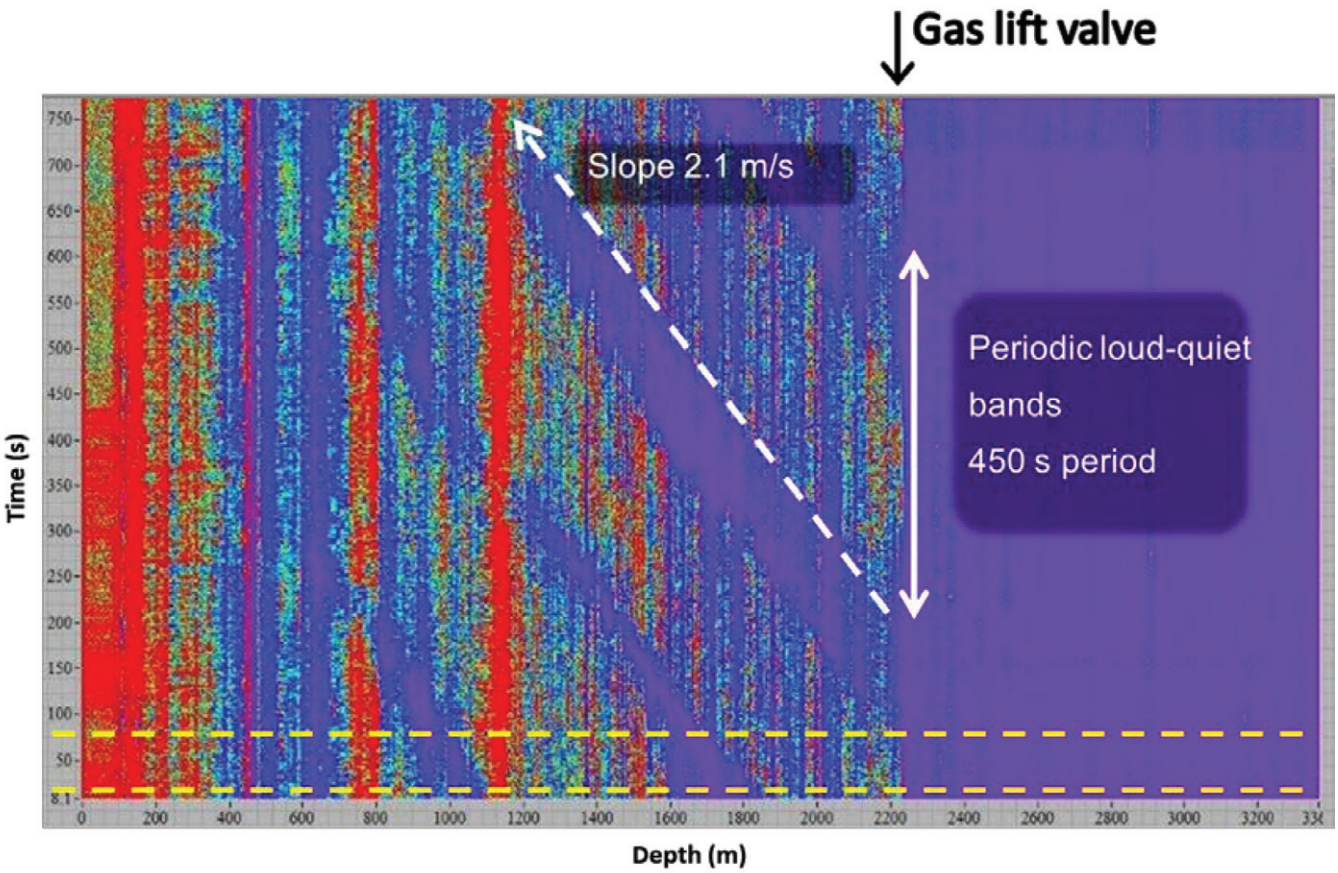

Fig. 7—Gas-lift diagnostics using distributed acoustic sensing.

Another application where distributed sensing offers benefit over conventional logging tools is leak detection. A sample of a gas leak detected using DAS is shown in Fig. 8. The leak was induced by bleeding down the annulus pressure by 300 psi to increase the pressure differential inside and outside of the tubing. The leak was only significant for just over a second after pressure bleed-down and would have been missed if a wireline logging tool was in the incorrect position at the point when the leak occurred. As the DAS covered the full wellbore depth it was possible to run the cable to TD and listen for leaks over the full depth range.

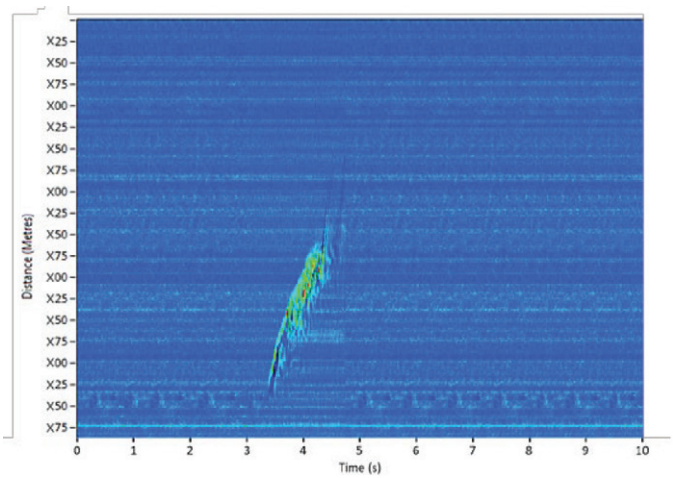

Fig. 8—A tubing leak detected using DAS.

Distributed sensors are also very good at measuring propagating effects, such as gas slugs or thermal perturbations, as they travel along the wellbore. The source of these events as well as their velocity can be useful indicators to perform wellbore diagnostics.

FLOW ALLOCATION USING DISTRIBUTED TEMPERATURE SENSING

The most well-known techniques for distributed sensing systems are those based on DTS. Temperature logging techniques have been in use since the early 1900s and were popular before the advent of more advanced production logging tools.

Before the well is put on production, the shut-in temperature survey represents the geothermal temperature as long as it has not been perturbated due to activities, such as mud-circulation during drilling, or placement of large volumes of injected fluids, as in hydraulic stimulation. In a producing well, an additional factor that may result in significant temperature changes at the inflow points is the Joule-Thomson effect (Hasan and Kabir, 1994). In such cases, inflows will not be at the same temperature as the geothermal temperature and special consideration needs to be given during the modeling of the temperature profile. As the fluid moves towards the wellhead, heat is transferred between the reservoir and the fluid. In case where the fluid is hotter than the reservoir, which is often the case in producing wells, as it loses heat to the surroundings as the ambient temperature of the solid material, i.e., the well components and the earth, are expected to be cooler. In case of cold fluid injection, the fluid gains heat from surroundings at it travels down the well and its temperature increases.

The temperature of the flowing fluid in the well is a function of several parameters, such as the intrinsic thermal properties of the fluid itself, well components, the earth, dimensions of the wellbore, the rate at which the fluid are produced, and the amount of time since the start of production. One of the most notable initial studies of the prediction of flowing wellbore temperatures in the oil and gas domain dates to 1962 (Ramey, 1962).

Ramey's study estimated the temperature of the injected fluid as a function of depth and time, assuming the fluid is injected at known rates and temperatures, and offered applications for several cases including cold- and hot-water injection as well as air and natural gas. Even though Ramey's work offered a satisfactory solution it had certain limitations. It only works for single-phase fluid, ignores the effects of friction and assumes a line-source well (Hasan and Kabir, 1994). A model that handles multiphase flow was later introduced by Hasan and Kabir (2002). Sagar et al. (1991) suggested a simplified model that handled multiphase flow, taking well dimensions into account but assuming the effects of the kinetic energy and Joule-Thomson effect being relatively small, and hence used a correlation (Shiu and Beggs, 1980) to account for those. A later study of Hasan and Kabir (1994) further improved the model, offering multiple solutions taking convective, conductive and radiative heat transfer into account and offering applications for various cases including heat transfer in offshore risers, single-phase and multiphase fluid flow in wellbores and injections. The main differentiator of this model from Sagar et al. (1991) is that it takes convection in the annulus into account.

It is possible to build a thermal model that handles multiphase-flow temperature models with multiple fluid entries by employing a robust thermal model of the types described above, incorporating thermal-mixing rules and accounting for the Joule-Thomson effect.

An example of such a model for a vertical wellbore is shown in Fig. 9. As we are modelling a vertical wellbore, the shut-in temperature can be seen to increase linearly from 20°C at the surface to 80°C at total depth (TD).

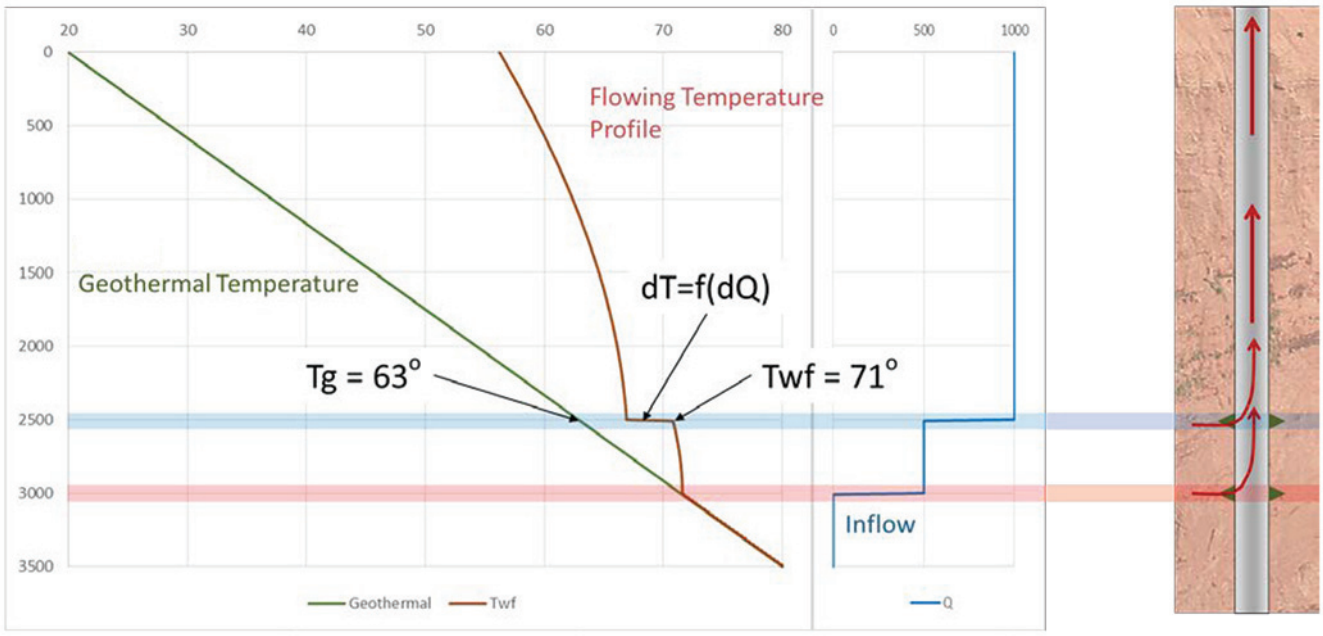

Fig. 9—Well flowing temperature behavior.

Flow from the lower perforation enters at the geothermal temperature of 72°C and travels up the wellbore, as shown by the red Flowing Temperature Profile. At the upper perforation the flow has lost 1°C due to conduction with the cooler wellbore surroundings. The heat loss per unit length can be calculated from Eqs. 1 and 2:

$$\frac{dTf}{dL} = -A\left[\left(T_f - T_e\right) + \frac{g}{g_c}\frac{sin\theta}{JC_{pm}A} - \frac{F_c}{A}\right], \quad (1)$$

where

$$A = \left(\frac{2\pi}{w_t c_{pL}}\right)\left(\frac{r_{ci}Uk_e}{k_e + \frac{r_{ci}Uf}{12}}\right). \quad (2)$$

A = coefficient, ft^{-1}
c_{PL} = specific heat of liquid, Btu/lbm-°F
c_{Pm} = specific heat of mixture, Btu/lbm-°F
g = gravitational acceleration, ft/sec^2
g_c = gravitational acceleration constant, ft/sec^2
Fc = correction factor
f = modified dimensionless heat conduction time function for long times for earth
J = mechanical equivalent of heat, ft-lbf/Btu
ke = conductivity of the formation, Btu/(D-ft-°F)
L = length of well from perforations, ft
rci = inside casing radius, in.
U = overall heat transfer coefficient, Btu/degF-hr-ft^2
w_t = total mass rate, lbm/sec
T_f = flowing fluid temperature, °F
T_e = surrounding earth temperature, °F
θ = angle of inclination, degrees

At the upper perforation in Fig. 9, flow enters at the geothermal temperature of 63°C and mixes with the warmer fluids, causing a local temperature drop of 4°C, before continuing to flow to surface. By measuring the local temperature drop, we can calculate the ratio of flow between the upper and lower perforations. If the flow from the upper perforation declines, the local temperature at the perforation depth would decrease, and conversely, if the flow from the upper perforation increases, the local temperature drop would increase. This describes the fundamental principle behind using temperature for mass flow-rate allocation.

Unfortunately, in multiphase-flow conditions, the model does not lead to a unique solution. Water has roughly twice the heat capacity of oil. If the water cut from the upper perforation increases, the local temperature drop would increase even if the rates remained constant. To explain this, we need to consider the thermal-mixing rule used to calculate the local temperature change, given by Eq. 3.

$$w_t c_m T_m = w_f c_{pf} T_f + w_{inflow} c_{pinflow} T_{inflow}, \quad (3)$$

where w is the mass flow rate, c the heat capacity and T the temperature. To better constrain the inflow model, it is clear that more information would be needed on the rate and fluid phase. The lack of phase information and nonunique solution to DTS inversion is normally the biggest challenge to interpretation based on DTS only. Some of the methods to identify phase based on DAS measurement will be discussed in the following sections.

While the previous example assumed that inflows were

at the geothermal temperature, this is often not the case, especially at high drawdowns or gas inflow. The temperature behavior at the perforations is mainly driven by the Joule-Thomson effect that is introduced by the pressure drop of the produced fluid between the reservoir and the wellbore. Temperature changes introduced by the Joule-Thomson effect can be explained by Eq. 4. Although Eq. 4 describes a single Joule-Thomson Coefficient (JTC), in practice the JTC will vary with composition, temperature and pressure.

$$\Delta T = \Delta P * JTC, \tag{4}$$

where ΔT is the temperature change cause by the Joule-Thomson effect in °F, ΔP is the pressure change in psi, and JTC is the Joule-Thomson coefficient in °F/psi.

As mentioned earlier, several flowing-well temperature models have been produced that take different combinations of processes and independent variables into account. One may think that picking a single model that considers the most number of factors is the best. However, complicated models may introduce longer run times and it would normally be recommended to select and customize a thermal model adapted to the well design.

DTS can also be applied to water-injection wells. While a full description of the methods is beyond the scope of this paper, a basic description of the principle is shown in Fig. 10. During injection, the bottomhole temperatures are normally significantly lower than the geothermal temperature as cool injection water travels from the surface to reservoir depth. This process cools a radius at the perforations around the wellbore, as shown in diagram on the left of Fig. 10. When the well is shut-in, the bottomhole temperature starts to return to its geothermal temperature, but zones that have taken significant volumes of fluid return to it more slowly. Applying methods, such as those developed in the 1950s (Nowak, 1953), it is possible to allocate total injected volumes to each reservoir interval.

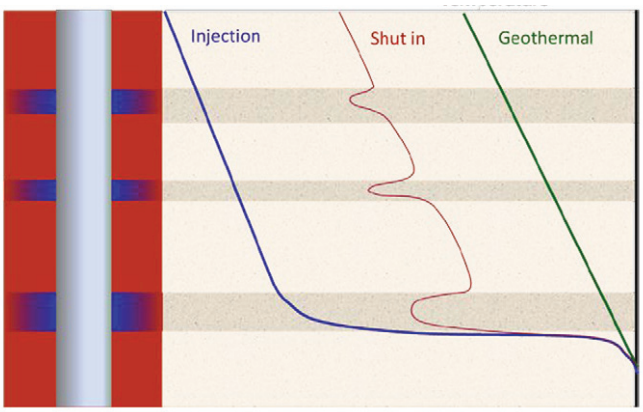

Fig. 10—Illustration showing the principle of a warm-back measurement in a water-injection well.

Field DTS data from a water-injection well that has been shut in for 24 hours is shown Fig. 11. The cooler temperatures of 120 to 130°F are from the injection period. The warm-back data were taken over the next 24-hour period. The bottom two perforations show almost no increase in temperature over this 24-hour shut-in period. We interpret this to mean these two intervals are taking the most water. The higher volume of injection water has cooled the near wellbore at these perforations more than other regions and these perforations are therefore warming back at a much slower rate.

In both the injection and production examples the interpretation is dependant on a strong understanding of the geothermal temperature. It is not always easy to measure or obtain the geothermal temperature from a production or injection well. There are, however, some practices that can be used to obtain a good understanding of the geothermal temperature. Where possible we would suggest installing a sump length with monitoring fiber below the lowest point of injection or production. This should be useful to measurement of geothermal temperature, and also a stable reference for quality control of DTS measurements. We would also suggest a period of monitoring before the well is first placed on production or injection. Even this pre-production temperature may not reflect actual geothermal temperature, due to disturbance by the drilling process, but it should provide a good reference.

SPEED OF SOUND MEASUREMENT BASED ON DISTRIBUTED ACOUSTIC SENSING

The previous section presented distributed temperature sensing as a powerful tool for mass-flow allocation but the difficulty in differentiating between oil and water production, based on just a well temperature profile is acknowledged. It will be shown in this section, how measuring propagating sound speeds can provide a complimentary tool, which can enable such differentiation. Discrete devices placed in a wellbore have been used to measure sound speeds at a single location (Kragas, 2002; Unalmis, 2015), however, DAS allows a continuous measurement of sound speed along a linear cable from surface to TD.

While the amplitude of the DAS response to an acoustic signal is governed by the DAS gauge length, its spectral content is also a direct function of the gauge length, as well as of the angle of incidence of that acoustic wave. With a 0° incidence, the acoustic wave travels in the same direction as the fiber installed along the pipe, and the smallest measurable wavelength is equal to twice the gauge length, due to the Nyquist theorem, which is illustrated in Fig. 12. When the acoustic signal's wavelength is equal to that of

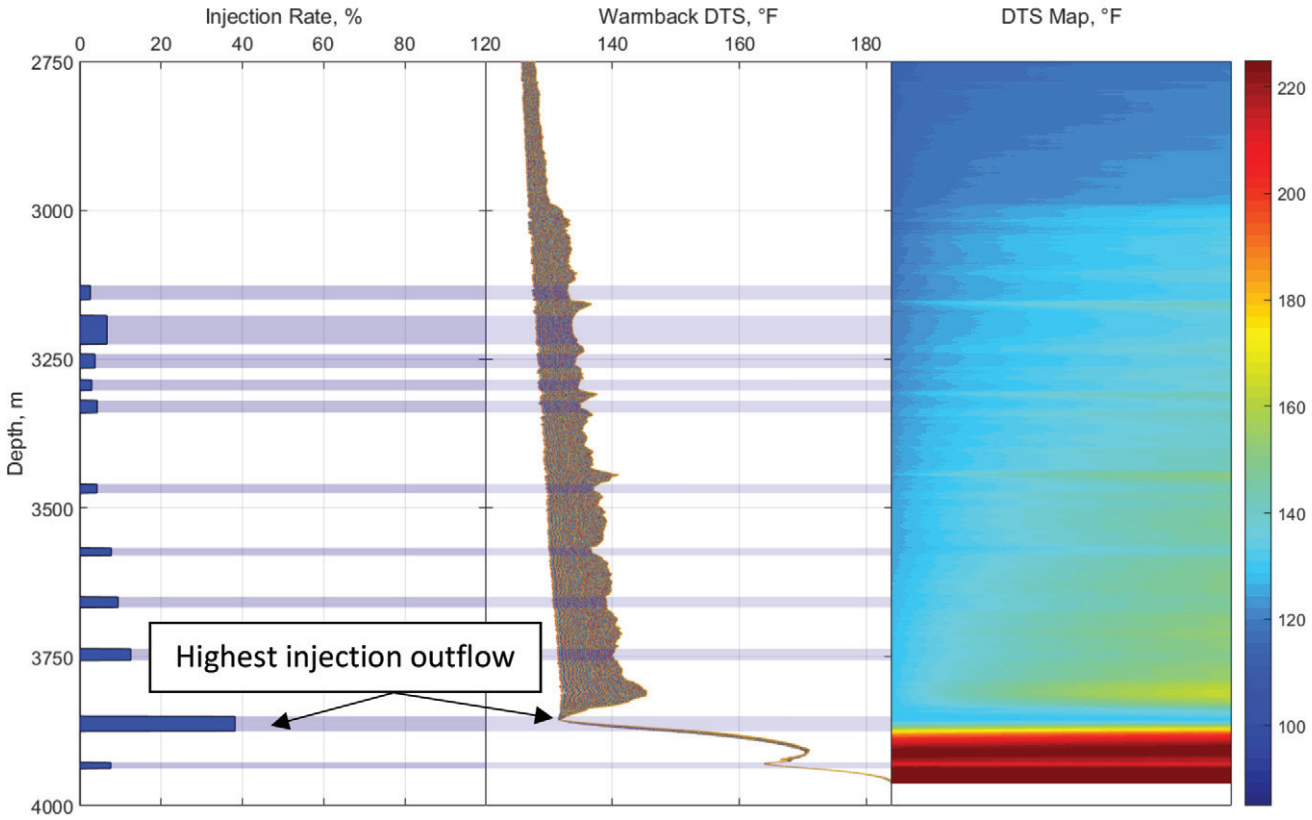

Fig. 11—A sample warm-back flow allocation analysis. The perforation depths are shown as blue horizontal bands. Where the temperature does not increase during injection shut-in, as seen in the center track, corresponds to high injection outflow. The injection allocation based on this warm-back response is shown on the left track.

the gauge length, as shown as the green wave in Figure 12, equal amounts of fiber are in tension and compression. In this case the average fiber elongation and therefore DAS output, is zero. A peak sensitivity wavelength can also be defined, which, to a very good approximation, is twice the DAS gauge length at 0° incidence. This case is shown as the red wave in Fig. 12.

If the direction of travel is rotated by 90°, such that the wave now approaches perpendicularly to the fiber, the entire acoustic waveform can be detected with highest sensitivity and with no loss in spectral information. This is typically the case during noise logging exercises at the perforations, where the waves propagate normal to the fiber. For the rest of the well, however, the sound travels along the fiber, as the pipe is acting as a waveguide and there will be a larger reduction in sensitivity.

Taking the average elongation into account, we can plot the DAS sensitivity as a function of the wavenumber (defined for simplification purposes here as the inverse of the wavelength) by performing a convolution of the signal and gauge length. The resulting sensitivity of a 10-m gauge length is shown in Fig. 13, where the cutoff wavelength is seen at 1/(10 m) and the peak sensitivity as seen at wavenumber 0.1 and peak sensitivity at 0.05.

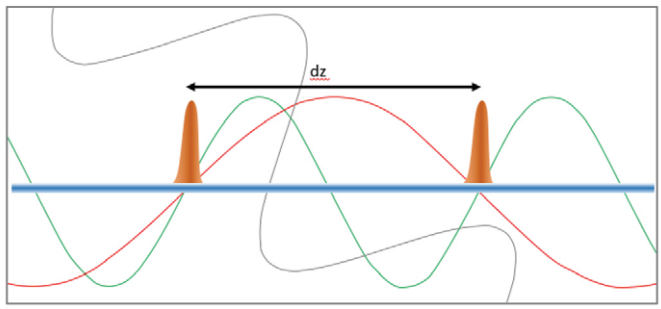

Fig. 12—Incidence of acoustic signals at 0° incidence with a wavelength of *dz* (green), 2×*dz* (red), and at 45° incidence with a wavelength of *dz* (grey).

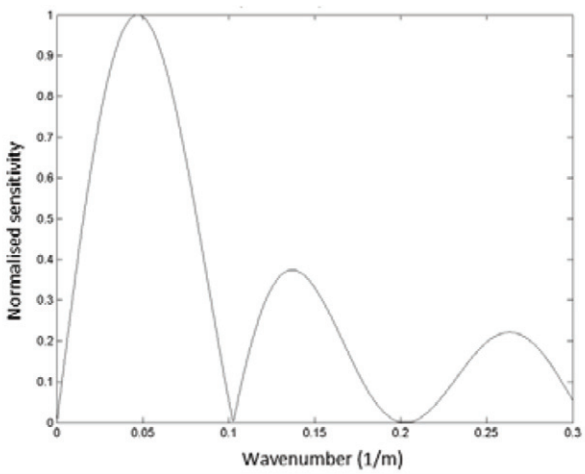

Fig. 13—Plot showing 10-m gauge length DAS normalized sensitivity versus wavenumber for 0° incidence angle.

One can also examine these results in the frequency domain by introducing the propagation speed of the incident wave. To a simple approximation, at a 0° incidence, the highest detectable frequency, f_{max}, of a propagating wave is given by Eq. 5:

$$f_{max} = \frac{c}{\lambda_{min}} = \frac{c}{2\,GL}, \quad (5)$$

where λ_{min} is the minimum measurable wavelength, c the speed of the traveling wave and GL the system gauge length.

In the case of single-phase water for example, the highest measurable frequency would be of 75 Hz for a system gauge length of 10 m and a sound speed of 1,500 m/s. In comparison, for single-phase gas, this frequency drops to 17.5 Hz at speed of sound of 350 m/s. This highlights the fact that an appropriate gauge length must be sought, depending on the application. A shorter gauge length would be a preferred choice for gas rather than for liquid wells.

Figure 14 illustrates sound speeds as a function of depth for both speeds traveling with and against the flow, in a trilateral well in Saudi Arabia (Xiao et al., 2013). The speed of sound was calculated by performing a 2D fast Fourier transform over a moving window of several distance-time waterfalls. A typical array length used for such calculation is 200 m, for a 10-m gauge-length DAS system. This length will be adapted depending on the fluid type and DAS spatial resolution. The change in completion size, from 3.5 to 4.5 in. at 6,000 ft (Fig. 14) is clearly marked by a change in sound speeds. A good understanding of the cable installation and coupling to its surrounding environment is therefore of high importance to be able to perform the correct interpretation.

Measuring the speed of sound not only allows for fluid composition trending, but also allows for the calculation of the fluid or gas flow speed along the wellbore via the Doppler shift. Fig. 15 shows how the flow speed was derived from both the upgoing and downgoing sound speeds at several locations along the wellbore in a gas well in the North Sea. The increase in average sound speed with depth directly relates to the increasing bottomhole temperature and pressure.

In a liquid-liquid system water has a sound speed of approximately 1,500 m/s and oil of approximately 1,300 m/s, exact values depend on the temperature and oil density. An increasing water holdup would result in an increasing sound speed, allowing the time and location of water breakthrough to be identified against the oil flow with lower sound speeds. The accuracy of this methodology was verified in a laboratory environment on a flow loop instrumented with a wrapped fiber section. A variation of 1% in the water-liquid ratio (WLR) of 1% could be detected by the corresponding change in sound speed. The relationship between sound speed and WLR is shown in Fig. 17.

In a gas-liquid system the response to gas breakthrough is even more dramatic, as sound speeds can drop from those of the liquid to below 200 m/s with only 1 vol% of gas, as shown in Fig. 16 (Kieffer, 1977).

BULK-FLOW MEASUREMENT USING DISTRIBUTED ACOUSTIC SENSING

Earlier work (Kragas, 2002) demonstrated that a fiber-optic based flowmeter can be used to independently determine both the water holdup and flow velocity. These meters were based on based on fiber-optic measurements but using Fiber-Bragg gratings and not DAS. Fiber-Bragg gratings are discrete marks that are written onto the fiber to create point strain sensors out of the fiber. A number of optical-grating sensors can be written onto a single fiber, allowing a quasidistributed strain-sensing system to be created (Kersey, 1997). As the DAS system is also a strain sensor, we can use the continuous distributed strain sensing to make a similar measurement of bulk-flow rate and sound speed.

Others (e.g., Finfer, 2015) have demonstrated how DAS can be used to measure small dynamic pressure variations induced by eddies within the flow. This eddy-flow velocity is a close approximation to the bulk-flow velocity and even allows the measurement of slip velocities in stratified two-phase flow conditions (Fig. 18). Figure 18a shows the processing of a single eddy measurement in a single-phase flow, while Fig. 18b shows two separate velocities for both the water and gas components of the flow.

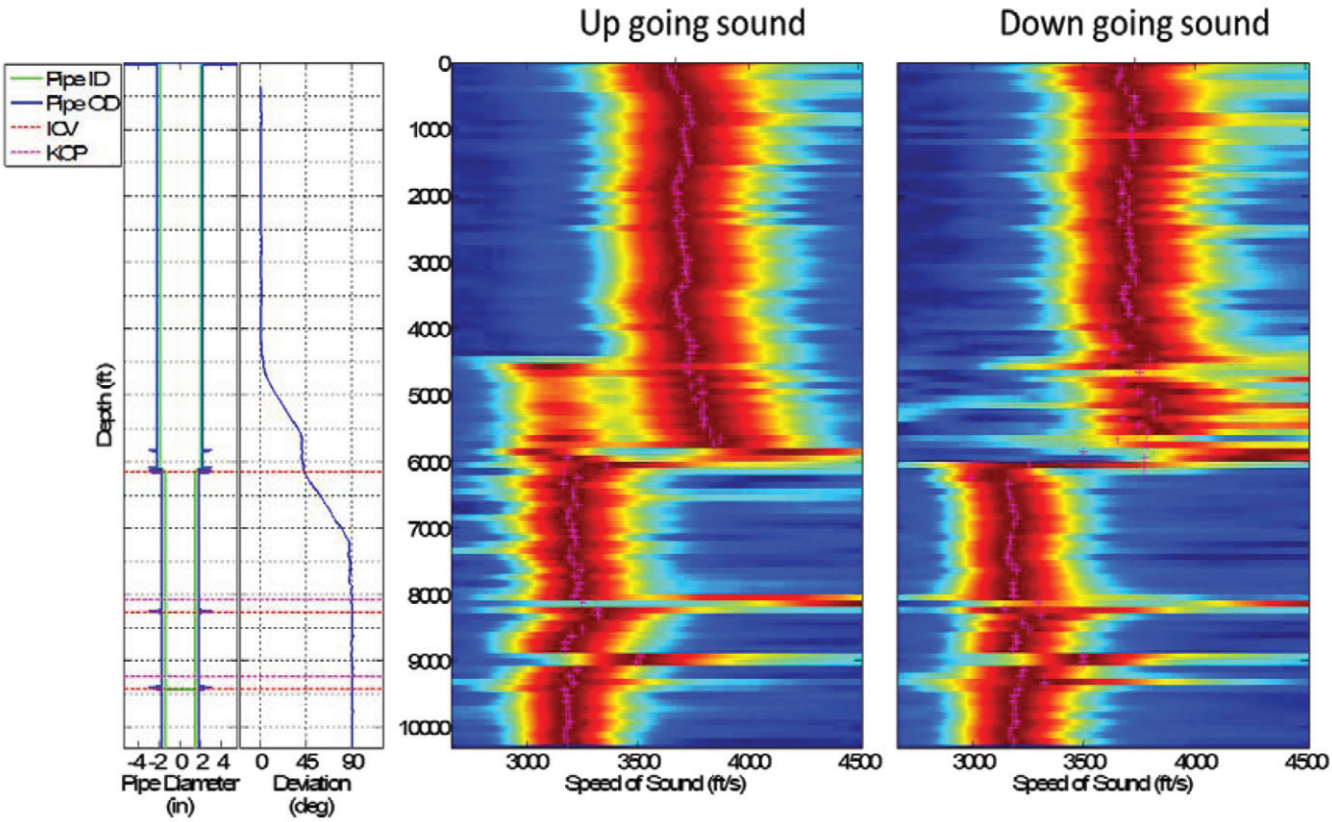

Fig. 14—Uphole and downhole speed of sound along the wellbore in a multilateral oil producer.

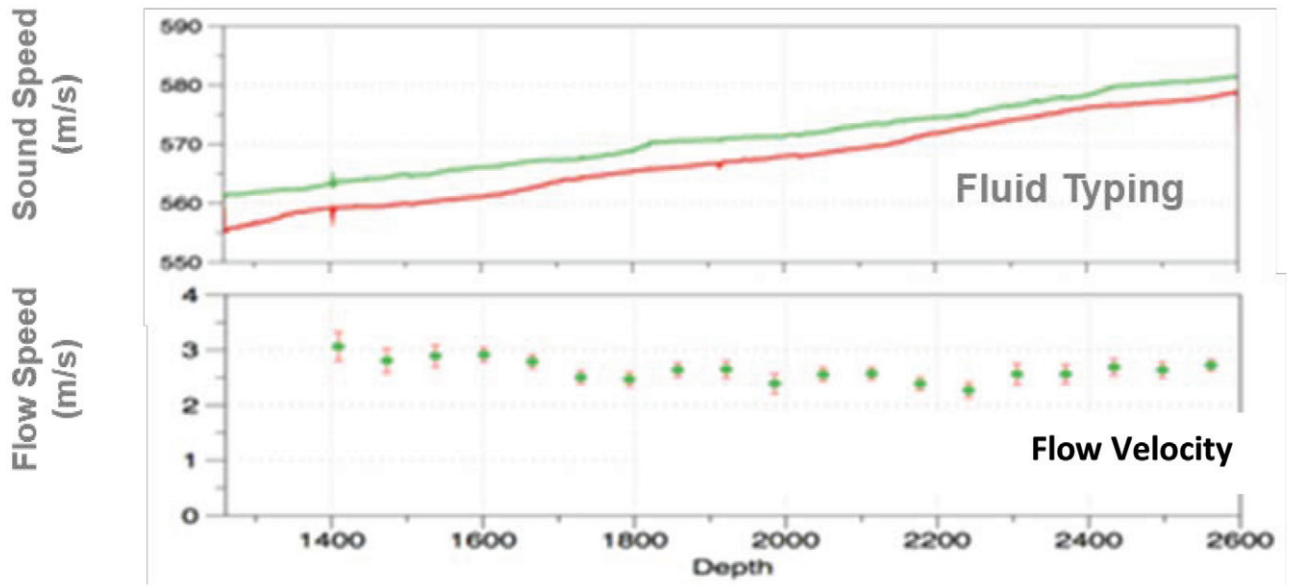

Fig. 15—The upper plot shows the measured uphole (red) and downhole (green) sound speeds at several points along a gas well. The sound speed in the direction of flow goes slightly faster due to the Doppler effect, and inversely, the sound speed against the direction of the flow goes slightly slower. In the lower plot, the flow speed, marked by the green dots and red error bars, can be derived directly from the Doppler shift.

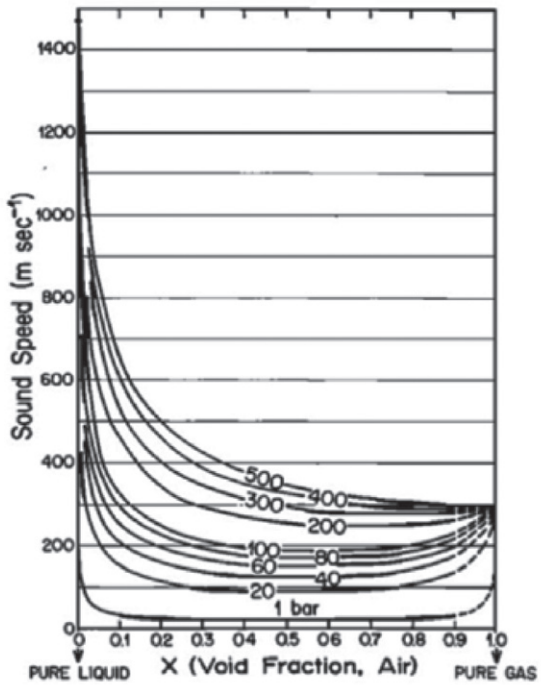

Fig. 16—Sound speed for differing gas-void fractions.

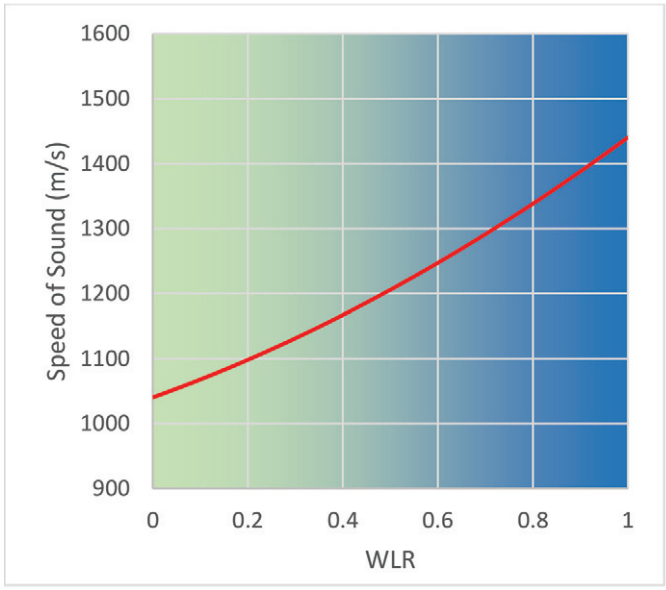

Fig. 17—Sound speed vs. oil-water ratio.

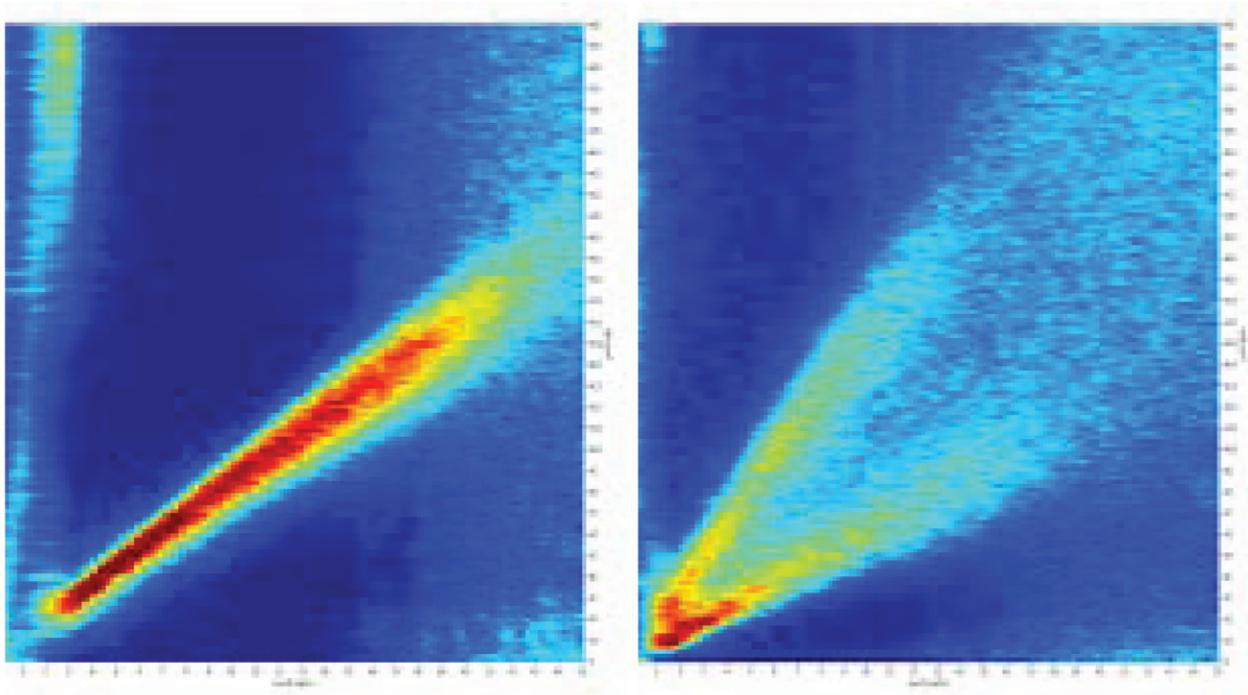

Fig. 18—DAS-based eddy measurements in (a) single-phase flow conditions, and (b) two-phase stratified flow.

Eddy measurements normally require a unique fiber-cable construction, but these can be readily accommodated within the envelope of a conventional logging tool. Designs of fiber-optic eddy-tracking logging tools are currently being field tested, and the results of these field tests will be presented in future publications.

The advantages of fiber over conventional tools, such as its high-temperature capability, have already been discussed, but fiber-based eddy measurements offer additional advantages over spinner arrangements. As there are no moving parts, the tool is not subject to wear, clogging or leaks. The lack of mechanical spinners also offers a significant advantage in wells where wax, asphaltenes or other types of debris are present.

FURTHER ADVANCES IN DISTRIBUTED ACOUSTIC SENSING PERFORMANCE

As with all new technologies, the early phase is subject to rapid and significant performance improvement. This is very much the case with DAS, where almost every year has seen improvement in measurement fidelity. In 2016, a new technological step was realized with the introduction of the Carina Sensing System. Improvements in the opto-electronic interrogator have been matched to an engineered optical fiber. It is the combination of these two improvements that is providing a new level of fidelity from the DAS system.

Most optical fibers are designed for long-range signal transmission and therefore aim to reduce any reflected or backscattered signal, this has limited the signal-to-noise ratio achievable with standard DAS systems. With Constellation fiber, brighter scatter centres have been introduced to the fiber core, allowing a stronger signal to return to the interrogator. The fiber is now a more integral part of the overall measurement system, allowing a 20 dB improvement in the signal-to-noise ratio of the measured acoustic signal. The fiber still retains the same mechanical dimensions as conventional fiber, which allows deployment in the same range of intervention methods described earlier in this paper.

A comparison between a standard DAS and one with enhanced fiber is shown in Fig. 19. Both systems were measuring on their respective fibers, within the same cable, at the same time. A vibrating source was providing the stimulation signal.

The waterfall at the top of Fig. 19 is showing distance on the x-axis and time on the y-axis. It is immediately apparent that the noise level with the enhanced fiber is significantly lower. A time slice is also taken along the red line on the waterfall diagram and plotted below. Again, the enhanced fiber has less noise and better amplitude stability than the system based on standard fiber.

The improved signal-to-noise ratio has a benefit in all areas of DAS interpretation. Noise sources, leaks and inflows are more easily detected with reduced detection thresholds. Sound speeds are measured more accurately over shorter distances. Flow speeds measured using eddy propagations are more accurate and have lower detectability thresholds.

DATA MANAGEMENT

Although there were some initial concerns about the data volumes generated by distributed sensing technology there has been significant progress in managing these datasets, accommodating both remote and connected wellsites.

Many operators have realized the benefits the technology has to offer, and are investing in the transmission, analytics and computing capability to handle fiber-optic datasets. Data lake lakes, which provide vast amounts of data storage

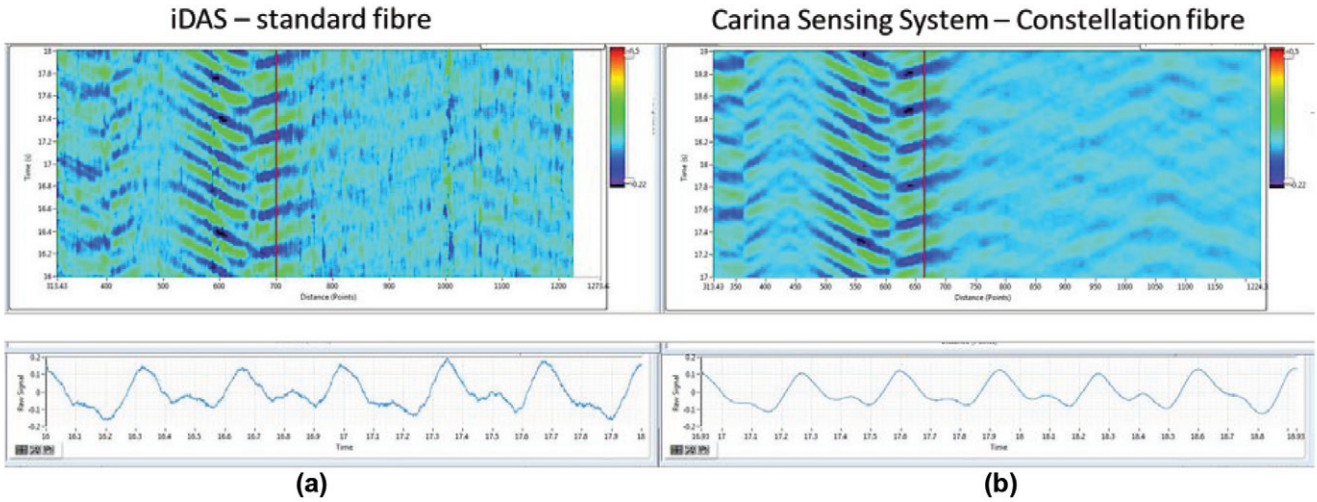

Fig. 19—Comparison between (a) a standard DAS measurement, and (b) one with Constellation fiber.

for acquired data, now exist in many organizations dealing with DAS. These are often combined with the distributed computing capacity offered by cluster computing.

Data volumes of terabytes per day are now being managed in real time, with processed data results delivered at the wellsite. By using high-speed fiber-based local area networks and compact high-performance computing (HPC) nodes at the wellsite, data streams can quickly be processed and displayed on a wellsite dashboard in real time. While we have described some of the physical models and processes in this paper there are also machine-based learning techniques being applied, to make both the overall process more efficient and the interpretation more complete.

CONCLUSIONS

In this paper, we have shown that fiber-optic technology offers unique methods of wellbore intervention when compared to traditional production logging tools. The combination of DTS and DAS data can be used to identify inflow locations, rates and phase. Processing of DAS measurements, i.e., using array-processing tools for the extraction of sound speeds and eddy velocity, is especially important for accurate inversion of measurement data to obtain rate and phase information. The information is acquired in real-time across the full length of the wellbore, making dynamic processes easier to capture and interpret.

ACKNOWLEDGEMENTS

The authors wish to thank the many staff in Silixa for their previous work on instrument development and interpretation methods described in this paper. We would also like to thank Morten Talgo of Capwell AS for the information and photos of the Capline synthetic rope intervention technology.

REFERENCES

Allanic, C., Frangeul, J., Liebeck, M., Carbonnier, B., Naldrett, G.J., Farhadiroushan, M., and Clarke, A. 2013, Distributed Acoustic Sensing for ESP Understanding and Surveillance, Paper SPE-167501 presented at the SPE Middle East Intelligent Energy Conference and Exhibition, Manama, Bahrain, 28–30 October. DOI: 10.2118/167501-MS.

Cobb C.C., and Schultz, P.K., 1992, A Real-Time Fiber Optic Downhole Video System, Paper OTC-7046 presented at the Offshore Technology Conference, Houston, Texas, USA, 4–7 May. DOI: 10.4043/6046-MS.

Finfer, D., Parker, T.R., Mahue, V., Amir, M., Farhadiroushan, M., and Shatalin, S., 2015, Non-Intrusive Multiple Zone Distributed Acoustic Sensor Flow Metering, Paper SPE174916 presented at the SPE Annual Technical Conference and Exhibition, Houston, Texas, USA, 28–30 September. DOI: 10.2118/174916-MS.

Hartog, A., 1983, A Distributed Temperature Sensor Based on Liquid-Core Optical Fibers, *Journal of Lightwave Technology*, **1**(3), 498–509. DOI: 10.1109/JLT.1983.1072146.

Hasan, A.R., and Kabir C.S., 2002, *Fluid Flow and Heat Transfer in Wellbores,* Society of Petroleum Engineers. ISBN: 978-1-5563-094-2.

Johannessen, K., Drakeley, B.K., and Farhadiroushan, M., 2012, Distributed Acoustic Sensing—a new Way of Listening to your Well/Reservoir, Paper SPE-149602 presented at the SPE Intelligent Energy International Conference, Utrecht, The Netherlands, 27–29 March. DOI: 10.2118/149602-MS.

Kersey, D.A., Davis, M.A. Patrick, H.J., LeBlanc, M., Koo, K.P., Askins, C.G., Putnam, M.A., and Friebele, E.J., 1997, Fiber Grating Sensors, *Journal of Lightwave Technology*, **15**(8), 1442–1463. DOI: 10.1109/50.618377.

Kieffer, S.W., 1977, Sound Speed in Liquid-Gas Mixtures: Water-Air and Water-Steam, *Journal of Geophysical Research Atmospheres*, **82**(20), 2895–2904. DOI: 10.1029/JB82i020p02895.

Kragas, T.K., van der Spek, A., and Al Hashmi, K.M., 2002, Field Trial of a Downhole, Fiber Optic, Two-Phase Flowmeter in PDO's Nimr Field, Paper SPE-78306 presented at the European Petroleum Conference, Aberdeen, UK, 29–31 October. DOI: 10.2118/78306-MS.

Li, X., Parker, T., Farhadiroushan, M., and Blacklaw,D., 2004, Evaluating a Concept of Using Distributed Optical Fiber Temperature and Strain Sensor for Continuous Monitoring of Casing and Completion Mechanical Deformation in Intelligent Wells, Paper OTC-16285 presented at the Offshore Technology Conference, Houston, Texas, USA, 3–6 May. DOI: 10.4043/16285-MS.

Nowak, T.J., 1953, The Estimation of Water Injection Profiles From Temperature Surveys, Paper SPE-953203-G, *Journal of Petroleum Technology*, **5**(8). DOI: 10.2118/953203-G.

Ramey, H.J., 1962, Wellbore Heat Transmission, Paper SPE-96, *Journal of Petroleum Technology*, **14**(4), 427–435. DOI: 10.2118/96-PA.

Sagar, R., Doty, D.R., and Schmidt, Z., 1991, Predicting Temperature Profiles in a Flowing Well, Paper SPE-19702, *SPE Production Engineering*, **6**(4). DOI: 10.2118/19702-PA.

Shatalin, S., Treschikov, V.N., and Rogers, A.J., 1998, Interferometeric Optical Time-Domain Reflectometry for Distributed Optical-Fiber Sensing, *Applied Optics*, **37**(24), 5600–5604. DOI: 10.1364/AO.37.005600.

Shiu, K.C., and Beggs, H.D., 1980, Predicting Temperatures in Flowing Oil Wells, *Journal of Energy Resources Technology*, **102**(1), 2–11. DOI: 10.1115/1.3227845.

Smolen, J., and van der Spek, A., 2003, *Distributed Temperature Sensing: A DTS Primer for Oil and Gas Production,* Shell International Exploration and Production (SIEP), publication EP 2003-7100.

Unalmis, H., 2015, The Use of Sound Speed in Downhole Flow Monitoring Applications, *Proceedings of Meetings on Acoustics*, **23**(1). DOI: 10.1121/2.0000069.

Xiao, J., Farhadiroushan, M., Clarke, A., Khalifa, Q., Mulhem,

A., Forero Reyes, H., Parker, T.R., Shawash, J., and Milne, H.C., 2013, Inflow Monitoring in Intelligent Wells Using Distributed Acoustic Sensing, Paper SPE-167447, SPE Middle East Intelligent Energy Conference and Exhibition, Manama, Bahrain, 28–30, October. DOI: 10.2118/167447-MS.

ABOUT THE AUTHORS

Garth Naldrett is the Chief Product Officer at Silixa. He has previously worked as Vice President of Monitoring and Control at Tendeka, founder and Managing Director of FloQuest and Fiber Optic Product Champion at Schlumberger. Garth holds a BSc in Electronic Engineering and MSc in Electrical Engineering from the University of Cape Town.

Cagri Cerrahoglu is currently a Production Petrophysicist at Silixa Ltd. Previously he had worked for the wireline segment of Schlumberger in various locations. Cerrahoglu's research interests include production petrophysics and production optimisation. Cerrahoglu holds a BSc from ITU and an MSc from Imperial College London both in Petroleum Engineering.

Veronique Mahue is a Lead R&D Engineer at Silixa, developing downhole flow monitoring solutions with distributed sensing. Veronique holds a PhD in Bioengineering from Imperial College, London, and a Masters of Engineering and Physics from the Grenoble Institute of Technology.